Korean J. Chem. Eng., **17**(5), 564-569 (2000)

Liquid-Liquid Phase Separation during Polysulfone Membrane Preparation

Je Young Kim, Hwan Kwang Lee* and Sung Chul Kim†

Center for Advanced Functional Polymers, Korea Advanced Institute of Science and Technology,
373-1, Kusong-Dong, Yusung-Gu, Taejon 305-701, Korea
*Department of Industrial Chemistry, Chungwoon University, #29, Namjang-Ri,
Hongsung-Eub, Hongsung-Gun, Chungnam 350-800, Korea
(*Received 10 May 2000 • accepted 9 August 2000*)

Abstract–The cloud point curves for a ternary system of PSf/NMP/water were determined by a titration method at 15 °C, 30 °C, 45 °C and 60 °C. A small amount of water (3-10 wt% water) was needed to achieve liquid-liquid phase separation and the temperature effect was not significant. The vitrification composition for the ternary system of PSf/NMP/water was determined by DSC measurements for various compositions. Cross-sectional membrane morphologies were examined by SEM (Scanning Electron Microscope) and surface morphologies by AFM (Atomic Force Microscope) varying the parameters including polymer concentration and bath compositions. It was observed that there were two different modes of phase separation during the formation of polysulfone membrane when the coagulation conditions were varied.

Key words: Phase Diagram, Phase Separation, Polysulfone Membrane, Vitrification, Atomic Force Microscope (AFM)

INTRODUCTION

Polysulfone (PSf) is widely used as a membrane material since it has excellent chemical resistance, mechanical strength, thermal stability and transport properties. The preparation of polymeric membranes usually involves the phase transition process, in which a homogeneous polymer solution undergoes phase separation into a polymer-rich phase and a polymer-poor phase by the exchange of solvent with nonsolvent in a coagulation bath. Phase separation continues to form the membrane structure until the polymer rich phase is solidified [Mulder, 1991]. Generally, solidification during phase separation may occur by gelation and/or crystallization of the polymer [Vadalia et al., 1994; Kim et al., 1999].

While the final morphology obtained during phase transition depends upon the kinetics as well as the thermodynamics of the phase separation, the equilibrium phase diagram and vitrification line for amorphous polymers are still a good tool for controlling the morphology and interpreting the membrane structure [Lau et al., 1991; Altena and Smolders 1982].

Asymmetric polymeric membranes prepared by the phase transition technique usually have either a top layer consisting of closely packed nodules or pores dispersed throughout the membrane surfaces. Many research groups are trying to explain the surface morphology with phase separation mechanism involved during the membrane preparation. Panar et al. [1973] were the first to report the existence of a nodule structure in the top layer of reverse osmosis membranes. Wienk et al. [1994] prepared Polyethersulfone (PES) Ultrafiltration (UF) membranes which had a top layer consisting of nodules, suggesting that the nodular structure was formed by spinodal demixing. Many authors have tried to gain a better insight into the fine structures of membranes by using microscopic techniques like SEM and AFM [Bessieres et al., 1996; Kim et al., 1999].

In this work, we are concerned with a thermodynamic analysis of a PSf/NMP/water system. We also present SEM and AFM images of PSf membrane which resulted from different phase separation mechanisms following spinodal decomposition and nucleation and growth of polymer poor phase.

EXPERIMENTAL

1. Materials

Polysulfone was Udel P-3500 purchased from Amoco Performance Products. The polymer had an $\overline{M}_n$ of 33,500 and an $\overline{M}_w$ of 50,800 obtained by size exclusion chromatography. The solvent was N-methyl-2-pyrrolidinone (NMP) purchased from Aldrich Chemical Co. Solvent was HPLC grade and used without further purification. Distilled water was used as a non-solvent.

2. Cloud Point Measurement

The cloud point curves were determined by a titration method at various temperatures of 15 °C, 30 °C, 45 °C and 60 °C. Thermostatted flasks with a rubber septum stopper were filled with 100 g of polymer solution. The distilled water was added into the binary solution by a syringe through a septum, while thorough mixing was applied by using a mechanical stirrer. Composition at the cloud point was determined by measuring the amount of water added when a visual turbidity was achieved.

3. DSC Measurement

Samples were prepared by weighing the appropriate amount of polysulfone, NMP and water in silver sample pans by using a micro-syringe. The amount of the polymer was about 8-10 mg. Pans were hermetically sealed and they were stored in a vacuum oven

†To whom correspondence should be addressed.
E-mail: kimsc@sorak.kaist.ac.kr
This paper was presented at The 5th International Symposium on Separation Technology-Korea and Japan held at Seoul between August 19 and 21, 1999

for at least two days at 210 °C to obtain a homogeneous solution. The sealed silver pan can endure 50 atm of inner pressure, and there was no measurable weight loss after heat treatment. A temperature of 210 °C was chosen because it is higher than the T_g of Polysulfone (190 °C). The DSC apparatus was a SEIKO model DSC 120 equipped with cooling accessories for subambient operation. All DSC runs were carried out with a heating rate of 10 °C per minute.

4. Membrane Preparation

Polysulfone was dried in a vacuum oven (80 °C) for 24 hours to remove absorbed water vapor before use and polysulfone was dissolved in NMP to form casting solution. The concentration was 20-30 weight percent. The solution was cast on glass plate at a thickness of 10 mils (250 μm) with a doctor blade and at room temperature. The polysulfone solution on glass plate was immediately immersed in the nonsolvent bath consisting of pure water and of 60/40 and 20/80 mixture of water/NMP by weight. After complete coagulation, both membranes were transferred to a fresh water bath for 1 hour for solvent exchange before being air-dried for at least 24 hours at room temperature. The air-dried membranes were further dried in a vacuum oven at 80 °C for 6 hours.

5. Tapping Mode AFM

Tapping mode AFM, which measures topography by tapping the surfaces with an oscillating tip, is similar to non-contact AFM, except that for tapping mode the vibrating cantilever tip is brought closer to the sample so that at the bottom of its travel it just barely taps the sample [Magonov et al., 1997]. The AFM used was Nanoscope III-a, a commercial device from Digital Instruments (USA). The scanner used was AS-130 (J-type), and a stiff crystal silicon probe was used for the tapping mode.

6. SEM

Surfaces of the samples were examined with a Philips SEM 535 M after gold coating. The used maximum coating rate was 20 nm/min and the coating period was 1.5 minutes.

RESULTS AND DISCUSSION

1. Cloud Point Curve

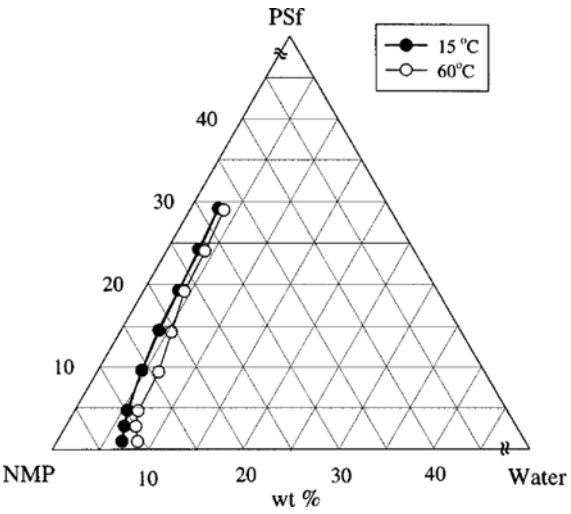

Fig. 1. Cloud point curve of PSf/NMP/water system at 15 °C and 60 °C.

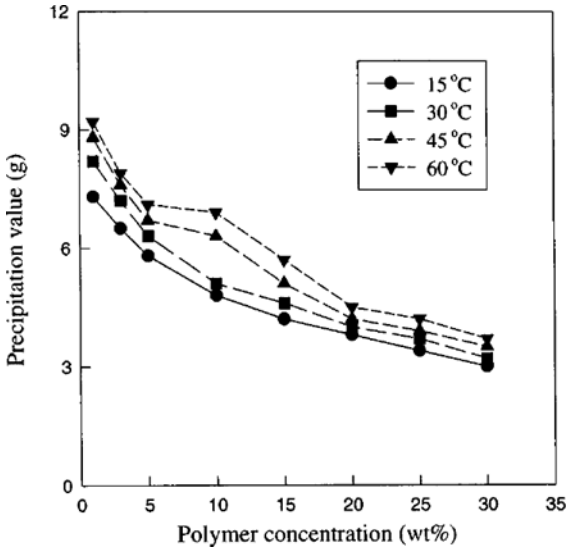

Fig. 2. Precipitation values of water as a function of polymer concentration (grams of water per 100 grams of polymer solution) for solutions of PSf-NMP at various temperatures.

Fig. 1 gives the experimental cloud point curves of the systems of PSf/NMP/water at 15 °C and 60 °C, which show the miscible region of polymer and solvent with water. We do not show the cloud point curves for 30 °C and 45 °C in Fig. 1 for the sake of clarity, but do show the effect of temperature in terms of precipitation value of water in polysulfone solutions (grams of water per 100 grams of polymer solution to obtain phase separation) in Fig. 2.

An obvious feature in Fig. 1 is that a small amount of water (3-10 wt% water) is needed to induce liquid-liquid demixing and the region of the homogeneous phase is enlarged slightly with increasing temperature. The effect of temperature on cloud point curve may indicate that the temperature dependence of interaction parameters is relatively small.

2. Vitrification Composition

The effect of solvent content on the glass transition temperature of polysulfone is shown in Fig. 3 up to 35 wt% of solvent content. The glass transition temperature drop with the addition of solvent is more pronounced in the concentrated region and is reduced in

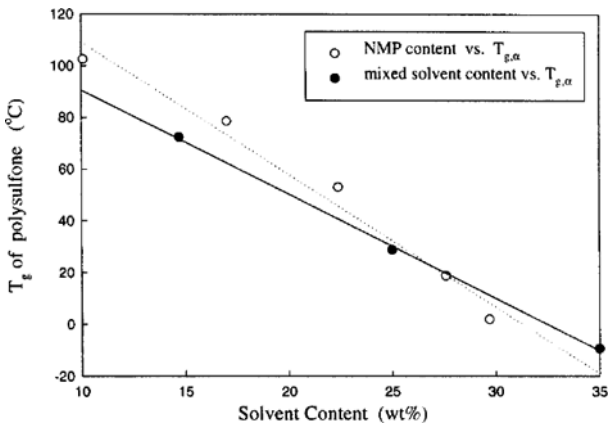

Fig. 3. T_g of PSf/NMP systems and PSf/NMP/water system in which the ratio of NMP to water is 94/6 in weight.

Table 1. The total solvent content (wt%) to reach the vitrification temperature in PSf/NMP and in PSf/NMP/water system (the ratio of NMP to water is 94/6 in weight)

Solvent \ T_g	15 °C	25 °C	30 °C	45 °C	60 °C
NMP	28.0	26.3	25.4	22.8	20.2
NMP : H_2O=94 : 6	28.6	26.2	24.9	21.2	17.5

*Interpolated value by 1st order regression.

the dilute region. Since membranes are generally prepared at room temperature, it is very important to know the vitrification composition in that temperature range. The slope of the pure solvent case is steeper than that of the mixed solvent case. From this figure we also estimate the vitrification composition at 25 °C, and it indicates very similar polymer concentration in both pure solvent and mixed solvent case.

Since a linear relationship between total solvent content and glass transition temperature of polysulfone was confirmed in the practical temperature range, one can obtain the composition of the solution at glass transition temperature, which is summarized in Table 1.

3. Cross-sectional Morphology

In Fig. 4, the cross-sections are shown of membranes prepared from 20 wt% PSf-NMP solutions immersed into a bath with varying water/solvent ratio. From (a) to (c) with increasing amount of solvent in the coagulation bath, we can observe a decreasing number of fingers, and the morphology is changed from finger-like to cellular structure. In higher magnification (lower parts of photographs), we can also observe increase of the cell size with increasing solvent content in the coagulation bath. This can be explained as follows. In case of (a), macrovoids are formed via spinodal decomposition mechanism and small cells around the macrovoids are formed via secondary nucleation and growth mechanism in the polymer-rich phase. The viscosity of the polymer-rich phase is high and results in smaller cell size. The addition of solvent to the coagulation bath decreases the rate of water inflow, thus tending to delay demixing. In case of (c), we cannot observe any macrovoids formed, which means that the primary phase separation mechanism is nucleation and growth of polymer poor phase. In this case the

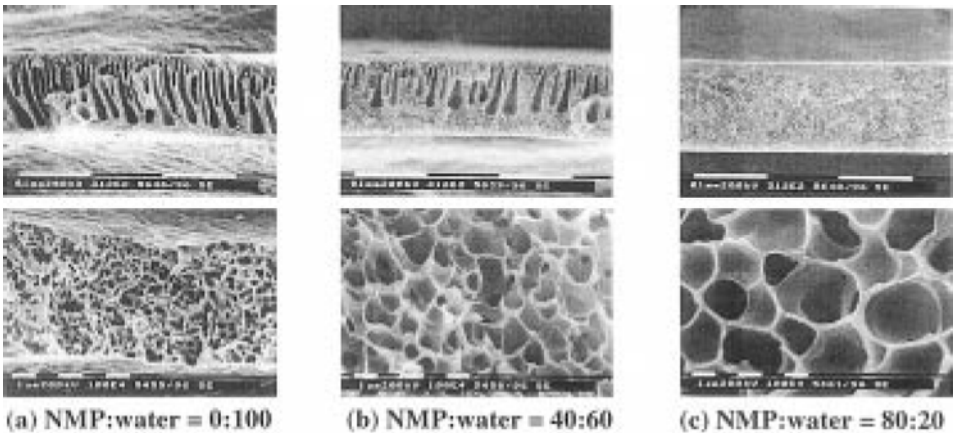

Fig. 4. SEM photographs of 20 wt% polysulfone membrane under different bath compositions [cross-section, ×300 (upper), ×10,000 (lower)].

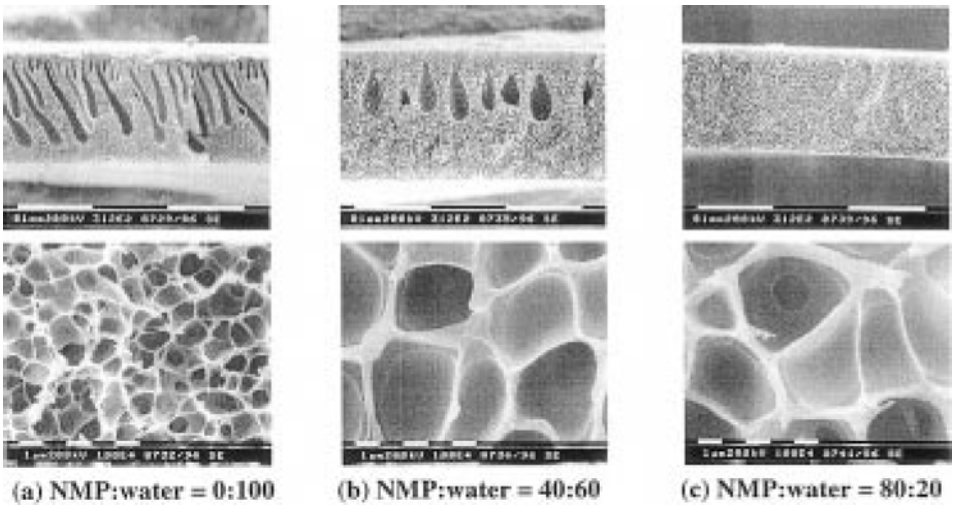

Fig. 5. SEM photographs of 30 wt% polysulfone membrane under different bath compositions [cross-section, ×300 (upper), ×10,000 (lower)].

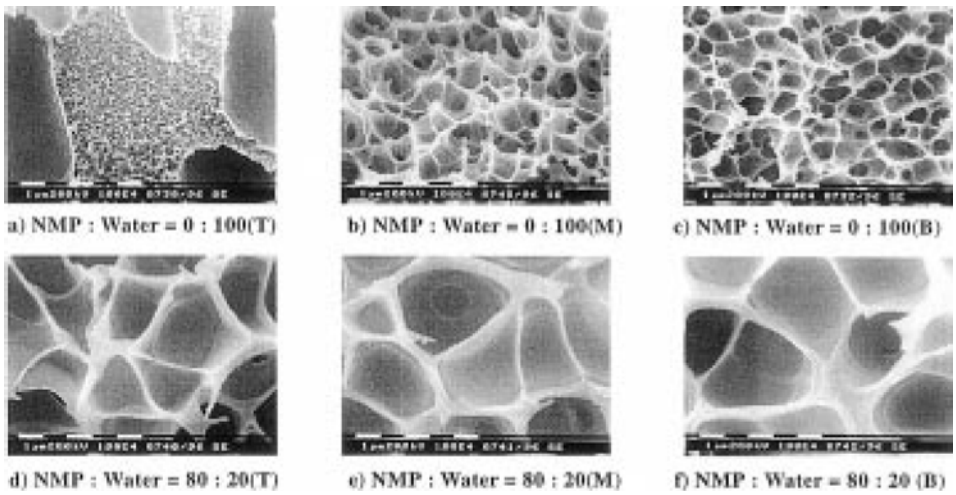

Fig. 6. SEM photographs of 30 wt% polysulfone membrane under different bath compositions with different locations (cross-section, ×10,000 T: Top, M: Middle, B: Bottom side of membrane).

solidification rate is slow so that cells can grow and coalesce each other, and results in open and large cellular structure.

In Fig. 5, cross-sections are shown of membranes prepared from 30 wt% PSf-NMP solutions immersed into a bath with varying water/solvent ratio. In this case the tendency of membrane morphologies is similar to Fig. 4. The number of macrovoids, however, decreases and cannot grow bigger than that of 20 wt% case resulting from the increase of the matrix viscosity and decrease of the diffusion rate of water.

In Fig. 6, cross-sections of different locations are shown of membranes prepared from 30 wt% prepared from solutions immersed into a bath with varying water/solvent ratio. In case of a water coagulation bath, the cell size of the upper region is very small compared to the lower side; this is caused by the steep gradient of polymer concentration near the membrane-bath interface which means very high polymer concentration near the interface but rather low polymer concentration in the bottom side. And in the case of 20/80 weight percent water/NMP coagulation bath, the gradient of polymer concentration gradually decreases and somewhat plateaus through the whole membrane thickness. This promotes the formation of a uniform porous sublayer. These features are in agreement with the experiments of Reuvers and Wijimans [Reuvers and Smolders, 1987; Wijimans et al., 1984].

Fig. 7 represent the schematic view of morphologies and involved phase separation mechanisms in case of instantaneous demixing. We believe that macrovoid are formed via spinodal decomposition mechanism and cellular structures are formed via nucleation and growth of polymer poor phase. The detailed procedure for macrovoid formation is as follows. The first layer (top layer of the membrane) was separated into polymer-rich and polymer-poor phases via spinodal demixing at the beginning of immersion. Then, the second layer was also separated into two phases; in this case spinodal decomposition occurs through the polymer-poor phase of the first layer. Third layer, fourth layer, and fifth layer etc. were separated by similar mechanism until the composition of the polymer-poor phase changed high solvent concentration, which leads to nucleation and growth mechanism. That results in highly elongated finger-like structures. Cells around the macrovoid are formed via nucleation and growth mechanism through secondary phase separation. The secondary phase separation means that after the primary phase separation occured, the polymer rich phase separated again into polymer-rich and poor phases via nucleation and growth mechanism. In that case the macrovoid (primary polymer-poor phase) acts as a local coagulation bath and the solvent concentration in the bath is high, which leads to nucleation and growth mechanism. Also the pores can grow further before solidification occurs and the coalescence of pores causes open and large pores.

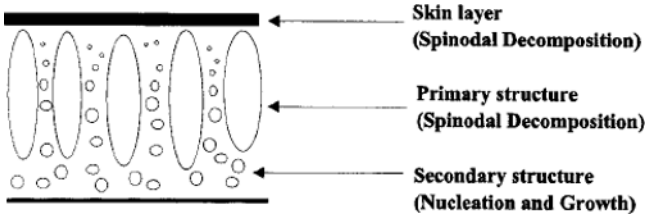

Fig. 7. Schematic representation of morphological structures and mechanisms involved in instantaneous demixing.

4. Surface Morphology

The surface structure of membranes prepared from 30 wt% PSf-NMP solutions immersed into a bath with varying water/solvent ratio imaged by AFM is shown in Fig. 8.

The view angle is 45 degree, which emphasizes the 3-dimensional feature of AFM images. Each figure has different *xy* scale, and the covering area of Fig. 8(a) is 200 nm×200 nm, and that of Fig. 8(b) is 3 μm×3 μm.

One can easily identify different surface structures in Fig. 8. Fig. 8(a) shows a typical nodular structure with interconnected cavity channels between the agglomerated nodules. It clearly shows the spinodal structure. Totally different surface structure exists in Fig. 8(b). There is no nodular structure, but large pores exist throughout the whole membrane surfaces. It is thought that these two structures originate from different phase separation mechanisms.

Polymeric membrane structure obtained from phase transition technique is closely related to phase separation mechanisms. Especially for amorphous polymer like polysulfone, liquid-liquid (L-L)

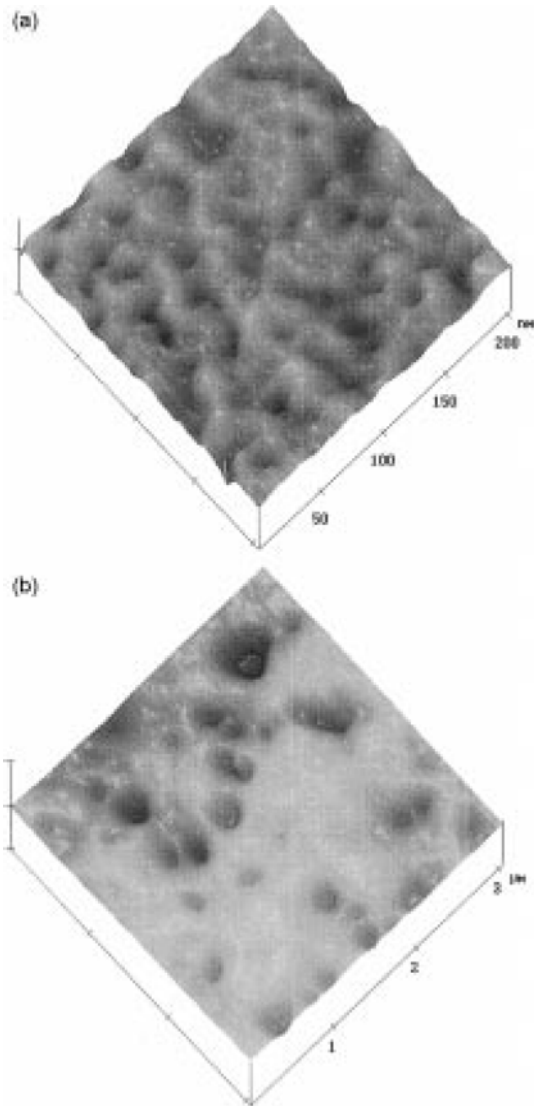

Fig. 8. Three-dimensional tapping mode AFM images of polysulfone membrane; prepared from 20 wt% solution immersed in (a) pure water coagulation bath, (b) 80/20 NMP/water coagulation bath.

phase separation is very important for determining the membrane morphology.

We presented two membranes that have totally different structures. The membrane prepared from pure water of the coagulation bath [Fig. 8(a)] showed a typical nodular structure with interconnected cavity channels between the agglomerated nodules on the membrane surface. This structure recalls the spinodal decomposition mechanism in which polymer-rich phase became nodules and polymer-poor phase is interstitial cavities on the top layer of the membrane. In this case, the spinodal decomposition maybe stopped instantly, resulting in the co-continuous structure because the solidification process is also very rapid due to high diffusion rate of NMP and water.

Membrane prepared from mixed nonsolvent bath [20/80 water/NMP in weight, Fig. 8(b)] showed a porous structure, and the morphology is believed to be the result of nucleation and growth of the polymer-poor phase. Thus, the polymer-poor phase became pores

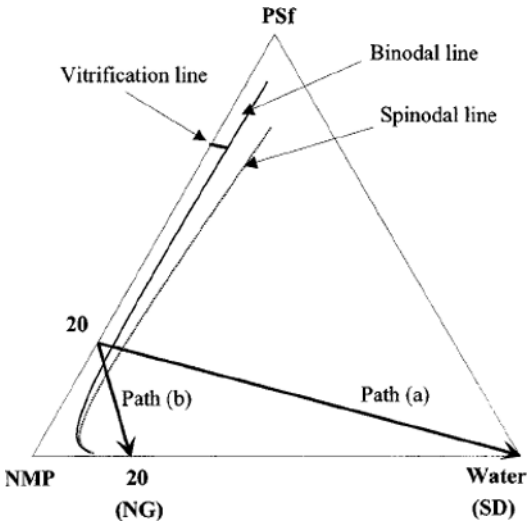

Fig. 9. Ternary phase diagram for PSf/NMP/water system showing binodal line, spinodal line and vitrification line. The diffusion trajectories near the surface region of two different cases are also indicated: path (a) represent for the case of immersed in pure water coagulation bath, path (b) for the 80/20 NMP/water coagulation bath.

and polymer-rich phase developed into the matrix. In this case, the nucleation and growth mechanism can progress for some period before solidification of polymer-rich phase because the solidification rate would be slow due to low diffusion rate of NMP and water. Phase diagrams of polysulfone/NMP/water system are shown in Fig. 9, which may provide the possible explanation of surface morphology in terms of phase separation mechanisms.

We are also carrying out calculations on the mass transfer to show the diffusion trajectory on the phase diagrams which will be reported in the future. The diffusion trajectories in Fig. 9 represent the calculated results in typical cases near the surface region with the parameters relevant to PSf/NMP/water system.

When a homogeneous solution becomes thermodynamically unstable, e.g. by the introduction of a non-solvent, the original solution undergoes phase separation by splitting up into two liquid phases of different composition called polymer-rich phase and polymer-poor phase. There are two kinetic ways for L-L phase separation to occur: either by nucleation and growth or by spinodal decomposition. Entering the metastable region, the area surrounded by the binodal and spinodal line, nuclei are formed in the polymer solution. These nuclei will grow into droplets until they touch each other and coalesce or until their growth stops by solidification of the surrounding polymer solutions.

The situation of path (a) in Fig. 9 would be realized if nonsolvent could diffuse very quickly and pass the spinodal line before nucleation could take place. For those compositions the solution is unstable with respect to infinitesimally small concentration fluctuations. The solution then separates spontaneously (by diffusion of molecules) into interconnected regions of high and low polymer concentration ending up in intertwined networks of phases with composition polymer-rich and polymer-poor [Cahn, 1968].

CONCLUSIONS

We determined the cloud point curves for a ternary system of PSf/NMP/water at various temperatures. An obvious feature in the phase diagram is that a small amount of water was needed to induce liquid-liquid phase separation and the region of the homogeneous phase is enlarged slightly with increasing temperature.

The vitrification curve for the ternary system of PSf/NMP/water was determined by DSC measurements with varying the compositions. The vitrification composition was 72.0 wt% of polysulfone and 28.0% of solvent at 15 °C and 79.8 wt% of polysulfone and 20.2% of solvent at 60 °C, respectively.

We observed the cross-sectional membrane morphologies with SEM (Scanning electron microscope) varying the parameters including polymer concentration and bath compositions. When we increase solvent content in water bath, we can observe that the occurrence of decreasing number of fingers and morphology is fully changed from finger-like type to cellular structure in case of 20/80 mixture of water/NMP by weight.

Atomic force microscopy (AFM) is an effective tool for investigating the surface structure of the membranes. Membrane prepared from pure water as a nonsolvent shows nodular structures of about 25 nm nodule size, which is believed to be the result from spinodal decomposition. Membrane prepared from mixed nonsolvent bath (20/80 water/NMP in weight) has a porous structure of mean radius of about 146 nm, and this morphology is the result of nucleation and growth of the polymer-poor phase.

REFERENCES

Altena, F. W. and Smolders, C. A., "Calculation of Liquid-Liquid Phase Separation in Ternary System of a Polymer in a Mixture of a Solvent and a Nonsolvent," *Macromolecules*, **15**, 1491 (1982).

Bessieres, A., Meireles, M., Coratger, R., Beauvillain, J. and Sanchez, V., "Investigations of Surface Properties of Polymeric Membranes by Near Field Microscopy," *J. Memb. Sci.*, **109**, 271 (1996).

Cahn, J. W., "Spinodal Decomposition," *Trans. of the Metal. Soc. of AIME*, **242**, 166 (1968).

Kim, J. Y., Kim, Y. D., Kanamori, T., Lee, H. K., Baik, K. J. and Kim, S. C., "Vitrification Phenomena in Polysulfone/NMP/Water System," *J. Appl. Polym. Sci.*, **71**, 431 (1999).

Kim, J. Y., Lee, H. K. and Kim, S. C., "Surface Structure and Phase Separation Mechanism of Polysulfone Membranes by Atomic Force Microscopy," *J. Memb. Sci.*, **163**, 159 (1999).

Lau, W. W. Y., Guiver, M. D. and Matsuura, T., "Phase Separation in Carboxylated Polysulfone/Solvent/Water Systems," *J. Appl. Polym. Sci.*, **42**, 3215 (1991).

Magonov, S. N., Elings, V. and Whangbo, M. H., "Phase Imaging and Stiffness in Tapping-Mode Atomic Force Microscopy," *Surf. Sci.*, **375**, 385 (1997).

Mulder, M. H. V., "Basic Principles of Membrane Technology," Elsevier, Amsterdam (1991).

Panar, M., Hoehn, H. H. and Herbert, R. R., "The Nature of Asymmetry in Reverse Osmosis Membranes," *Macromolecules*, **6**, 777 (1973).

Reuvers, A. J. and Smolders, C. A., "Formation of Membranes by Means of Immersion Precipitation," *J. Memb. Sci.*, **34**, 45 (1987).

Vadalia, H. C., Lee, H. K., Myerson, A. S. and Levon, K., "Thermally-Induced Phase-Separation in Ternary Crystallizable Polymer-Solutions," *J. Memb. Sci.*, **89**, 37 (1994).

Wienk, I. M., Boomgaard, Th. V. D. and Smolders, C. A., "The Formation of Nodular Structures in The Top Layer of Ultrafiltration Membranes," *J. Appl. Polym. Sci.*, **53**, 1011 (1994).